Received: 8 January 2018 | Revised: 24 June 2018 | Accepted: 7 July 2018

DOI: 10.1111/iep.12282

ORIGINAL ARTICLE

WILEY INTERNATIONAL JOURNAL OF Experimental Pathology

Adaptive growth changes in the liver remnant are affected by the size of hepatectomy in rats

Michelle Meier[1] | Kasper Jarlhelt Andersen[1] | Anders Riegels Knudsen[1] | Jens Randel Nyengaard[2] | Stephen Hamilton-Dutoit[3] | Frank Viborg Mortensen[1]

[1]Section for Upper Gastrointestinal and Hepato-Pancretico-Biliary Surgery, Department of Surgical Gastroenterology, Aarhus University Hospital, Aarhus, Denmark

[2]Section for Stereology and Microscopy, Department of Clinical Medicine, Centre for Molecular Morphology, Centre for Stochastic Geometry and Advanced Bioimaging, Aarhus University, Aarhus, Denmark

[3]Institute of Pathology, Aarhus University Hospital, Aarhus, Denmark

Correspondence: Kasper Jarlhelt Andersen, MD, PHD, Department of Surgical Gastroenterology, Section for Upper Gastrointestinal and Hepato-pancretico-biliary surgery, Aarhus University Hospital, Noerrebrogade 44, building 1C, DK-8000 Aarhus, Denmark (kasperjarlheltandersen@gmail.com).

Funding information
Villum Foundation

Summary

In this study we investigated the dynamics of hepatocyte hyperplasia and hypertrophy in rats subjected to increasing sizes of partial hepatectomy (PH). A total of 104 rats were randomized according to the size of PH. On postoperative days (PODs) 1, 3 and 5, blood was drawn and the remnant liver removed for stereological analysis. Liver parameters and regeneration rate were significantly affected by size of PH. On POD 1, hepatocyte volumes had increased significantly in all PH groups. On POD 3, all groups showed hepatocyte volumes approximating baseline. On POD 5, hepatocyte volumes were significantly lower in PH (90) than in baseline, sham and PH (30) rats. Increasing hepatocyte proliferation was not observed following PH (30). Following PH (70), cell proliferation was significantly elevated on PODs 1 and 3, and following PH (90) on PODs 3 and 5. In conclusion, general hypertrophy of hepatocytes after different size of PH was followed by hepatocyte proliferation only in the liver remnant of PH (70) and PH (90).

KEYWORDS

hepatic surgery, hepatocyte hyperplasia, hepatocyte hypertrophy, liver regeneration, posthepatectomy liver failure

1 | INTRODUCTION

Partial hepatectomy (PH) remains an important treatment option for both primary and secondary liver malignancies, both of which are increasing worldwide.[1,2] Up to 75% can be resected in healthy humans leaving a future liver remnant (FLR) of 25%. Exceeding this limit may result in posthepatectomy liver failure (PHLF), which is a severe condition, associated with a high morbidity and mortality.[3] In rats, the minimal size of FLR is approximately 10%.[4,5]

Evolution has equipped the healthy liver with a unique ability to regenerate in response to loss of parenchyma, such as is seen after PH. Initiation, progression and termination of liver regeneration are complex processes involving a magnitude of pathways. Regeneration terminates rather precisely when the normal liver-to-body weight ratio is restored, that is, the organ has regained its original size. The overall regulator orchestrating these complex processes can be termed the hepatostat, and much is still to be learned about how it functions.[6] The size of an organ is the result of both cell number and cell size.[7] Recently, it has been proposed that liver regeneration is in most cases the result of both hepatocyte hyperplasia and hypertrophy.[8]

Meier and Andersen shared first-authorship.

© 2018 The Authors. International Journal of Experimental Pathology © 2018 International Journal of Experimental Pathology

After minor PH of 30% in mice, it seems that hypertrophy alone is responsible for the restoration of lost liver mass. When performing larger PH of 70%, it has been shown that hypertrophy precedes proliferation and, at termination of liver regeneration, half of the regeneration is due to hypertrophy, the other half being due to cell proliferation.[8] However, the relationship between hypertrophy and proliferation and how it is affected by minimal size FLR (MSFLR) and PHLF has not been studied.

In this study we aimed, by unbiased stereological methods, to investigate the regenerative dynamics of hyperplasia and hypertrophy in the rat liver following increasing PH (30%, 70% and 90%), the latter being close to the limit for the FLR.

2 | METHODS

2.1 | Animals

Healthy 10-week-old male Wistar rats (M&B Taconic, Eiby, Denmark) with a mean weight of 206 g (range: 145-239) were housed in standard animal laboratories, with the temperature maintained at 23°C, an artificial 12-hour light-dark cycle, and with free access to food and water. The rats were kept in the animal facilities until the end of the experiment.

2.2 | Ethical approval

The experimental protocol was approved by the Danish Animal Research Committee, Copenhagen, Denmark (license number: 2012-15-2934-00591). Animals received care in accordance with the *Guide for Care and Use of Laboratory Animals* published by the US National Institutes of Health.

2.3 | Study design

In total, 104 male Wistar rats were randomized in blocks of 5 according to the size of partial hepatectomy to be performed: PH (30) (n = 24), PH (70) (n = 24), PH (90) (n = 24), sham (n = 24) and baseline (n = 8). Each group (not baseline) was further block-randomized into 3 subgroups according to the day of euthanization: postoperative days (PODs) 1, 3, and 5 (n = 8 per group)(Figure 1) in accordance with a previous study conducted by this study group presenting the natural history of liver regeneration in rats subjected to PH (70) PH.[9]

2.4 | Surgical procedure

The surgical procedure was performed as described in an earlier publication by our group.[10] In brief, when performing PH (30), the left lateral lobe (LLL) was resected. In PH (70), the LLL and the ML were resected. In PH (90), the right lobes (RL), ML and LLL were resected, leaving only the two caudate lobes (posterior caudate lobe (PCL), anterior caudate lobe (ACL)) intact.[5]

2.5 | Tissue sampling

In the morning of PODs 1, 3, or 5, the rats were anaesthetized and a laparotomy was performed through the previous incision. Blood samples were collected from the heart by cannulation. Animals were then euthanized by cervical dislocation under anaesthesia. The remnant liver was removed, and the PCL was fixed in phosphate-buffered formalin for 24-48 hours.

2.6 | Biochemical analyses

Alanine aminotransferase (ALT), alkaline phosphatase (AP), haptoglobin (HP) and bilirubin (BR) levels were measured using Modular P (Roche Diagnostics, Mannheim, Germany).

Prothrombin-proconvertin ratio (PP) was measured using automated coagulation analyser Sysmex CS2100i (Sysmex©, Tokyo, Japan).

2.7 | Regeneration rate

Liver weight dynamics were evaluated by the hepatic regeneration rate (RR) as described previously by our group[10]:

$$RR = \frac{LW_{remn}/BW_{euth}}{ELW_{pre\,op}/BW_{pre\,op}} \times 100$$

$BW_{pre\ op}$ = body weight preoperatively. BW_{euth} = body weight at euthanization.

The preoperative estimated liver weight ($ELW_{pre\ op}$) was calculated from the resected liver weight as

$$ELW_{pre\,op} = \frac{LW_{resect}}{\text{size of PH}} \times 100.$$

2.8 | Stereology

2.8.1 | Tissue preparation

The formalin-fixed PCL was cut into 2.25-mm-thick parallel slabs using a razor blade tissue slicer and placed with the same side up before being embedded in paraffin.[11] 30-μm sections were cut from each paraffin-embedded block, providing systematic uniformly random sampling (SURS) sections for immunohistochemical staining and further analysis.[12]

2.8.2 | Immunohistochemistry

The Ki-67 antigen was used as marker of cell proliferation.[13] The 30-μm-thick tissue sections were deparaffinized

and boiled in Tris-EGTA buffer, pH 9, for heat-induced epitope retrieval. Monoclonal mouse anti-rat Ki-67–specific antibody (clone MIB-5, isotype IgG1; Dako, Glostrup, Denmark) diluted at 1:20 was used as the primary antibody. Sections were incubated with the primary antibody for 4 days at 4°C and washed, and positive signals were visualized using the EnVision þ horseradish peroxidase–labelled anti-mouse detection system (Dako). The sections were counterstained with haematoxylin.

To visualize the hepatocyte cell membrane, 30-μm-thick paraffin sections were deparaffinized. Following an in-house protocol, monoclonal NCL-β-catenin (Novocastra™, Newcastle, UK) with added diluent (Dako, Glostrup, Denmark) 1:50 was used as the primary antibody (incubation time: 32 minutes). The sections were counterstained with haematoxylin (incubation time: 8 minutes).

2.8.3 | Quantitation

All sections were blinded to the examiner. Stereological analysis was performed using an Olympus BX50 microscope modified for stereology with a motorized stage (Märzhäuser Wetzlar MFD, Germany) and a digital camera (Olympus DP70) connected to a computer running newCast version 6.4.1.2240 (Visiopharm, Hørsholm, Denmark).

Hepatocellular proliferation was quantified as described in detail previously.[10] In brief, the optical fractionator method was used to count Ki-67 positively stained hepatocyte nuclei in each tissue section. From this, we were able to calculate the total number of Ki-67–positive cells in each PCL.

Hepatocyte volume was measured using the isotropic planar rotator[14] applied on each of the disector-sampled hepatocytes (Figure 2 A-C). Microscopy was performed using a 60× oil objective lens (Olympus PlanApo 60x/1,40 Oil, Japan). In each section, a mean of 25 counting frames ($75 \times 55\ \mu m^2$) and an average of 50 hepatocytes were sampled for hepatocyte mean volume estimation (V_i). Positive hepatocytes were defined as a hepatocyte with a clear beta-catenin–stained cell membrane (dark-red) and a counterstained (grey) oval nucleus in focus (Figure 2 A-C). The software made the calculation of the individual hepatocyte volume V_i. To get the mean volume of hepatocytes in a section (V_{mean}), the following formulas were used:

$$V_{\text{mean}}(\log(V_i)) = \sum \log((V_i) \times (t_i/h_i)) / \sum (t_i/h_i)$$

$V_{mean}(log(V_i))$ is a logarithmic calibrating constant, t_i is the section thickness and h_i is the optical disector height.

$$V_{mean} = 10^{V_{mean}(log(V_i))}$$

The comparison of V_{mean} between the rat groups assumes equal shrinkage of hepatocytes in the paraffin sections.

2.9 | Statistical analysis

Data were tested with regression analysis using STATA v.13.1 (StataCorp, College Station, TX, USA) and presented as mean values given with a 95% confidence interval (CI). P-values < 0.05 were considered significant.

3 | RESULTS

3.1 | Mortality and morbidity

In total, ten animals were excluded before evaluation (four rats, found dead; six rats, euthanized because of General Distress Score (GDS) ≥ 10). The distribution was as follows: PH (70) on POD 3: one rat; PH (90) on POD 3: five rats; and PH (90) on POD 5: four rats. None of the autopsies revealed identifiable cause of morbidity or mortality. To fill up the groups (n = 8), the excluded animals were replaced in an unbiased, randomized manner.

3.2 | Body weight

On POD 1, a weight loss was observed in all groups. Later in the study period, on POD 3 and POD 5, body weight was significantly lower in the PH (90) group compared with all other groups ($P < 0.001$).

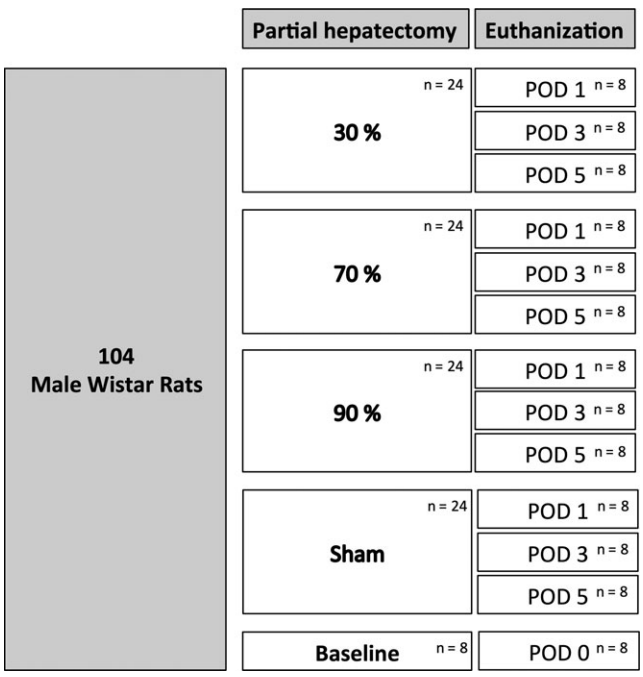

FIGURE 1 Study design: 104 male Wistar rats randomized into 5 groups according to the type of hepatectomy. Further randomization by time of euthanization: postoperative days (POD) 1, 3, and 5

3.3 | Liver-specific biochemistry

The biochemical dynamics are shown in Table 1. ALT levels were elevated after operation on POD 1 in all PH groups with the highest levels seen according to the increasing size of PH. On POD 3 and POD 5, all levels had declined to baseline with no difference between groups. (Table 1). BR was significantly elevated in the PH (90) group compared with all other groups on POD 1 ($P < 0.001$) and POD 3 ($P < 0.001$), before returning to baseline level on POD 5. After PH (90), PP dropped dramatically on POD 1 compared with all other groups ($P < 0.001$). At POD 5, PP was nearly normalized for all groups.

3.4 | Regeneration rate

RR following PH (90) increased significantly throughout the postoperative period with a RR of 82.2% (CI: 73.0; 91.3) at POD 5; significantly comparable with PH (30) (mean: 88.5, CI: 79.2; 97.9) and PH (70) (mean: 91.6, CI: 82.3; 100.9) at POD 5 ($P \geq 0.104$) (Table 2).

3.5 | Hepatocyte proliferation

No significant increase in hepatocyte division was observed following PH (30) compared with sham-operated rats. After PH (70), the number of Ki-67–positive cells was significantly elevated on POD 1, followed by a peak on POD 3. The number of Ki-67–positive cells declined to baseline levels on POD 5. In the PH (90) group, the response was delayed, with no increase in Ki-67–positive cell profiles on POD 1. However, on POD 3 and POD 5, cellular division was significantly increased compared with sham animals. Raw mean values are presented in Table 2.

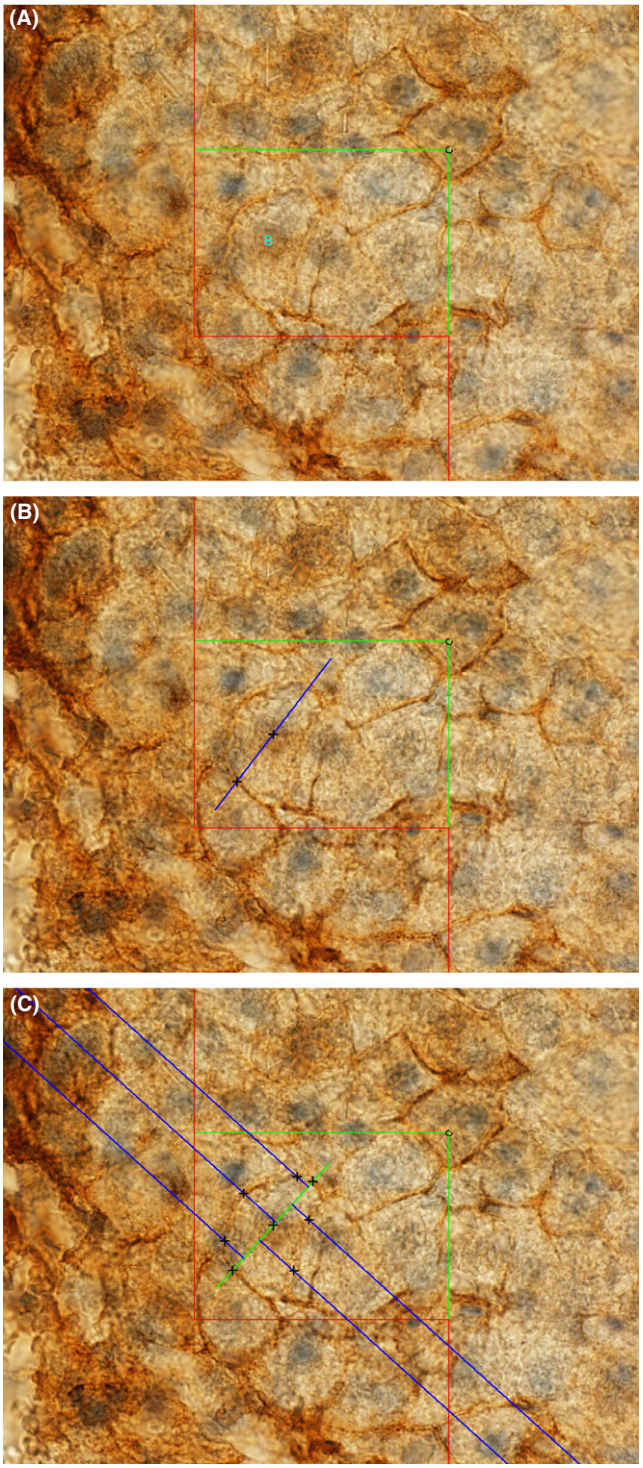

FIGURE 2 Beta-catenin–stained, thick (30 μm) paraffin section presenting the steps involved in measuring the volume of a hepatocyte by the planar rotator. The counting frame is displayed (75 × 55 μm^2); red and green lines are, respectively, exclusion and inclusion lines. The universal sampling rule states that a particle is sampled if it is entirely contained within the counting frame or if it touches an inclusion line without touching an exclusion line (14). In the present study, the object of interest was a hepatocyte with a clear beta-catenin–stained cell membrane (dark-red) and a counterstained (grey) oval nucleus in focus; the sample unit was the nucleus (A). From the top of the section, the microscope was focused 2 μm down, disregarding otherwise includable hepatocyte nuclei to avoid distortion and irregularity from the surface, as well as lost caps. Subsequently, hepatocyte nuclei coming in to focus when focusing the microscope down through the disector height (12 μm) were sampled according to the sampling rule. The planar rotator was applied as follows: through the middle of the nucleus, the longest axis of the hepatocyte (A) was marked. Intersections between the longest axis and the hepatocyte cell membrane were marked defining the cell "height" (B). The software generated uniform, random and parallel test lines perpendicular to the longest hepatocyte cell axis (C). Intersections between these test lines and the hepatocyte cell membrane were marked (C), defining the distance of the intercepts at both sides of the axis. The software calculated the volume of the hepatocyte [Colour figure can be viewed at wileyonlinelibrary.com]

TABLE 1 Liver-specific biochemistry. Mean (95% CI)

	30% partial hepatectomy			70% partial hepatectomy		
	POD 1	POD 3	POD 5	POD 1	POD 3	POD 5
Alanine aminotransferase, U/L	288 (198,378)	52 (44,60)	47 (39,55)	614 (269,959)	79 (60,98)	44 (37,50)
Alkaline phosphatase, U/L	230 (196,264)	103 (170,217)	220 (181,261)	423 (374,471)	376 (310,442)	218 (184,252)
Bilirubin, μmol/L	<5.0 (-)	<5.0 (-)	<5.0 (-)	<5.0 (-)	5.1 (4.8,5.4)	<5.0 (-)
Haptoglobin, g/L	0.37 (0.27,0.48)	0.43 (0.29,0.57)	0.31 (0.25,0.36)	<0.17 (0.16,0.18)	0.34 (0.24,0.45)	0.44 (0.32,0.56)
Prothrombin-proconvertin ratio	0.33 (0.30,0.36)	0.32 (0.30,0.33)	0.32 (0.30,0.34)	0.20 (0.18,0.23)	0.28 (0.25,0.31)	0.31 (0.24,0.37)

	90% partial hepaectomy			Sham			Baseline
	POD 1	POD 3	POD 5	POD 1	POD 3	POD 5	Pre-OP
Alanine aminotransferase, U/L	2034 (1652,2416)	136 (98,173)	51 (39,62)	65 (13,117)	44 (34,54)	48 (43,52)	34 (29,37)
Alkaline phosphatase, U/L	707 (569,844)	723 (560,886)	327 (281,372)	187 (146,227)	177 (147,207)	182 (150,213)	230 (190,269)
Bilirubin, μmol/L	49.3 (32.4,66.1)	11.6 (8.2,15.0)	<5.0 (-)	<5.0 (-)	<5.0 (-)	<5.0 (-)	<5.0 (-)
Haptoglobin, g/L	<0.17 (-)	0.21 (0.12,0.30)	0.42 (0.25,0.59)	0.45 (0.37,0.52)	0.29 (0.23,0.35)	0.35 (0.27;0.43)	<0.17 (-)
Prothrombin-proconvertin ratio	0.07 (0.06,0.09)	0.23 (0.20,0.25)	0.29 (0.25,0.32)	0.41 (0.37,0.44)	0.34 (0.32,0.36)	0.36 (0.32,0.41)	0.36 (0.33,0.38)

TABLE 2 Raw mean values by group of hepatocyte volume, total number of proliferating hepatocytes, prothrombin-proconvertin ratio and regeneration rate

		Hepatocyte volume μm^3	Total number of proliferating hepatocytes E^{-5}	Prothrombin-proconvertin ratio	Regeneration rate %
PH (30)	POD 1	5762 (5100,6423)	10.6 (4.67,16.6)	0.33 (0.30,0.36)	83.2 (73.4,93.2)
	POD 3	4984 (4608,5360)	9.14 (4.05,14.2)	0.32 (0.30,0.33)	83.5 (75.0,92.1)
	POD 5	5238 (4839,5637)	15.4 (10.5,20.2)	0.32 (0.30,0.34)	88.5 (79.2;97.9)
PH (70)	POD 1	6787 (6257,7317)	80.3 (46.7,114)	0.20 (0.18,0.23)	55.7 (50.6,60.8)
	POD 3	5060 (4696,5424)	132 (109,155)	0.28 (0.25,0.31)	79.9 (72.0,87.8)
	POD 5	4888 (4286,5489)	20.7 (7.95,33.3)	0.31 (0.24,0.37)	91.6 (82.3,101)
PH (90)	POD 1	7035 (6546,7523)	6.19 (3.17,9.21)	0.07 (0.06,0.09)	33.0 (29.7,36.3)
	POD 3	4691 (4271,5111)	252 (228,276)	0.23 (0.20,0.25)	64.2 (52.0,76.4)
	POD 5	4247 (3681,4814)	128 (68.5,186)	0.29 (0.25,0.32)	82.2 (73.0,91.3)
Sham	POD 1	4960 (4331,5589)	0.32 (0.21,0.43)	0.41 (0.37,0.44)	NA
	POD 3	5034 (4486,5581)	0.36 (0.15,0.56)	0.34 (0.32,0.36)	NA
	POD 5	5005 (4357,5654)	0.54 (0.33,0.76)	0.36 (0.32,0.41)	NA
Baseline		5247 (4726,5767)	7.23 (5.14,9.32)	0.36 (0.33,0.38)	NA

PH, partial hepatectomy; POD, postoperative day.
Values are given with a 95% confidence interval.

3.6 | Hepatocyte volume

On POD 1, hepatocyte volume was greater in the three PH groups compared with the sham group. The largest hepatocyte volumes were found with increasing size of PH (Table 2) with significant differences between sham and the PH groups: (PH (30): $P = 0.026$; PH (70): $P < 0.001$; PH (90): $P < 0.001$), and between PH (30) and PH (70)

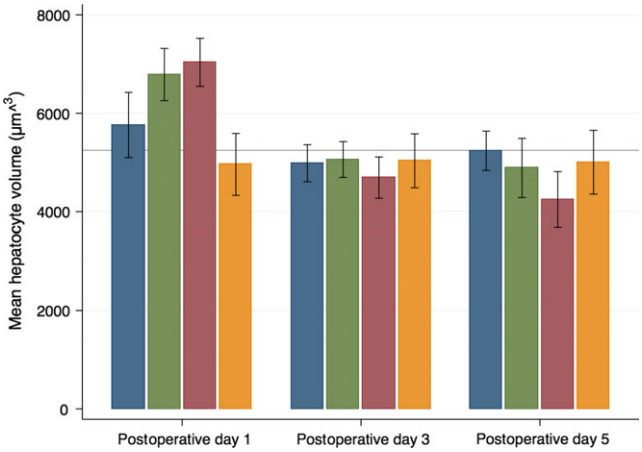

FIGURE 3 Mean hepatocyte volume by size of hepatectomy pre- and postoperative with 95% CI. Blue line: PH (30); green line: PH (70); red line: PH (90); orange line: sham; and grey line: baseline [Colour figure can be viewed at wileyonlinelibrary.com]

($P = 0.004$), and between PH (30) and PH (90) ($P = 0.001$). On POD 3 and POD 5, all groups showed hepatocyte volumes approximating baseline levels, however, with a significant difference on POD 5 between baseline and PH (90) ($P < 0.001$), sham and PH (90) ($P = 0.032$), and PH (30) and PH (90) ($P = 0.004$). Dynamics of mean hepatocyte volume for all groups are shown in Figure 3.

As depicted in Figure 4, data on hypertrophy of the hepatocytes were related to the proliferation of the hepatocytes, and the hepatocyte function judged by PP and the RR. The maximum mean hepatocyte volume was reached by PH (90) at POD 1, whilst maximum proliferation was reached by PH (90) at POD 3. During the early postoperative period, hepatic function in the PH (90) group, as measured by PP, was significantly reduced compared with all other groups ($P < 0.001$). The raw mean values for each parameter are presented in Table 2.

4 | DISCUSSION

In this experimental rat study, we demonstrate that the regenerative dynamics of hepatocyte volume and proliferation differs with the extent of PH. Following PH (30), only hepatocyte hypertrophy is induced, whilst hepatocyte hypertrophy after PH (70) and PH (90) is followed by proliferation.

At POD 1 after different size of PH, we found increasing hepatocyte volume in all three PH groups. The increase was proportional to the size of PH, however, not significantly different between PH (70) and PH (90). Miyaoka et al investigated hepatocyte size in mice after PHs of 30% and 70%.[8] They found that hepatocyte volume increased 1.5-fold after both types of PH. Unfortunately, they did not include mice undergoing 90% PH in their study. There are several possible explanations for the discrepancy between their results and the results in the present study. Firstly, they conducted their experiments in mice and not rats. Secondly, they estimated hepatocyte volumes at POD 2 and POD 5. Thirdly, they used an indirect method (an imaging cytometric approach) for hepatocyte volume estimation.[8] We believe that the unbiased stereological methods we used in our study are superior, as they allow very precise determination of both cell size and number, as has been demonstrated in studies of many other organs.[15]

At POD 5, hepatocyte volume following PH (30) and PH (70) approached baseline levels. In the group of PH (90), however, hepatocyte volume was further reduced below baseline values. One explanation for this could be that proliferation in the PH (90) group takes place at such a high rate that the newly formed hepatocytes are unable to synthesize enough cytoplasm to obtain the same volume as mature cells. This is, however, speculative, as investigation into the matter has not been reported in the literature.

With decreasing hepatocyte volume in all PH groups in the later postoperative period, the remaining hepatocytes of PH (70) and PH (90) proliferated. Notably, the inducement

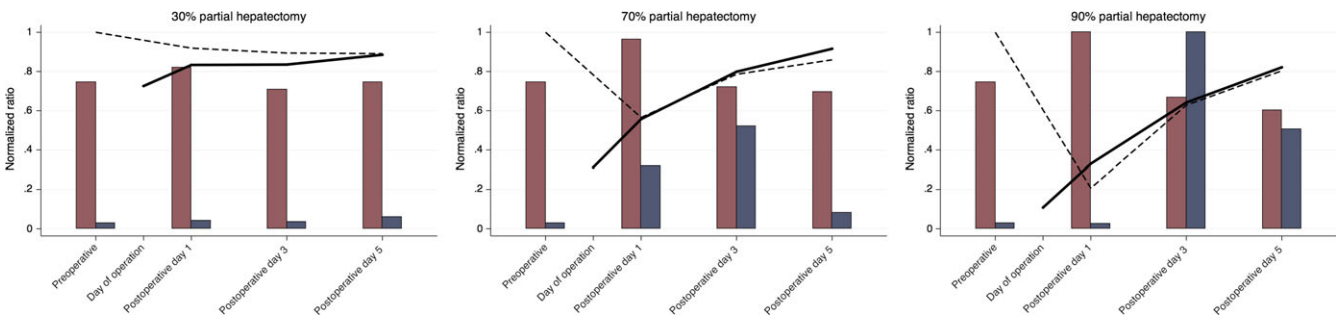

FIGURE 4 Hypertrophy and proliferation of the hepatocytes normalized to the maximum potential (90% PH POD 1 resp. POD 3) in relation to the regeneration rate and liver function (PP) by size of hepatectomy pre- and postoperative. Red bar: normalized mean cell volume; blue bar: normalized number of Ki-67–positive hepatocytes; black line: regeneration rate; and dashed line: prothrombin-proconvertin ratio normalized to baseline [Colour figure can be viewed at wileyonlinelibrary.com]

of proliferation was counterbalanced between the two groups; an inducement at POD 3 after PH (90) was delayed compared to the increase at POD 1 following PH (70). For both groups, a proliferative peak was seen at POD 3, in parallel to a decreasing hepatocyte volume. We suggest that the division of each hepatocyte may be an obvious and simple explanation for the reduction in hepatocyte volume.

In this study, we also assessed liver regeneration and liver remnant function, by calculating the RR, and by measuring PP, respectively. In the PH (30) group, liver resection had no major impact on either RR or PP. However, in the PH (70)- and PH (90) groups, hepatectomy had a major impact on both parameters. Thus, PP decreased on POD 1 to 60% and to 20% of initial values in the PH (70)- and PH (90) groups, respectively. This suggests impaired synthetic capacity of the liver remnant, especially in the PH (90) group. Subsequently, PP increased in both groups resulting in nearly normal function on POD 5. RR increased steeply in both the PH (70)- and PH (90) groups, starting on POD 1 and continuing until POD 5. These results are comparable with those reported by Inderbitzin D et al.[16] In their study on mice, they found that relative liver weight increased proportionally to the amount of parenchyma resected.[16] In our study, the dynamics of the curves for RR and PP in all resected groups were nearly identical, emphasizing the need for a normal synthetic activity to allow the liver to regenerate.

A simple explanation for liver dysfunction is most likely the highly reduced number of hepatocytes. Even though the functional capacity of each hepatocyte is fully optimized, this seems insufficient to maintain normal liver function. Hepatocytes need to be able to pass nutrients and gasses in and out of the cell in order to maintain homeostasis. Most of these processes occur passively along a concentration gradient. However, concentration gradients in the cytoplasm are not as great as those seen across the cell membrane, thus slowing down diffusion within the cell. Speculatively, an increase in cytoplasmic volume may in this sense have a negative influence on cell function.

As demonstrated by Kim RD et al, swelling of hepatocytes seems to stimulate activation of intracellular transcription factors leading to proliferation.[17] Our study indicates that swelling and hypertrophy have to exceed a certain threshold to induce proliferation. This speculation is based on our results showing that a maximal volume increase of 1.2-fold after PH (30) was not followed by a proliferative response, whereas a fold increase of 1.4 after both PH (70) and PH (90) was followed by hepatocyte proliferation.

We are the first to study hypertrophic and proliferative changes after the extensive PH (90). We used the proven PH model first described by Higgins & Anderson in 1931[18] and believe that the extended PH (90)-model mimics liver failure when evaluated at POD 1 (high BR and low PP).

As already stated, a major strength of our study is that we are the first to use unbiased stereological methods to assess adaptive changes in hepatocytes after increasing size of PH. Unlike standard pathological evaluation of liver pathology, quantitative information about a three-dimensional structure is obtainable from 2D tissue samples in an unbiased and randomized manner (Ref:[11]: A review of state-of-the-art stereology… + Boyce RW et al[19]: Design-based stereology: introduction to…).

A weakness of the study is the selection of rats, that is, ten animals were excluded before evaluation, four being found dead and six being euthanized because of GDS $\geq$ 10. All the excluded rats had an autopsy performed. In no case did this reveal an identifiable cause of morbidity or mortality. Nine of the excluded rats belonged to the PH (90) group, and all of them were replaced. In this sense, there is a selection of rats evaluated after 90% PH, that is, only rats not dying of PHLF or for other reasons were included in the study. It would of course also have been interesting to include rats dying of PHLF in our analysis. Unfortunately, this was not possible.

Many different methods have been proposed to evaluate hepatic function.[20] In this study, we used the PP as a marker of the liver's synthetic function[21,22] and BR as a marker of liver excretory function. We chose these biochemical markers for evaluating liver function as they are often used and widely accepted in a biochemical definition of liver failure with high BR and low PP. Preferably, such indirect biochemical markers of liver function are a supplement to direct rat liver function assessment such as the well-established tests of galactose elimination capacity (GEC) and capacity of urea-nitrogen synthesis (CUNS) (Hansen and Poulsen[23]: The capacity of Urea-N…). A bigger range of liver function assessments was, however, not the primary aim of this study.

Overall, in the study of Miayoka et al, they are proposing a revised model of liver regeneration with a first response to the loss of liver mass where hepatocytes enlarge which is sufficient for the loss of 30%. In the case of PH (70), hypertrophy is not sufficient to explain why hepatocytes in a second response proliferate. Overall, our findings support this proposal. However, our results do suggest that the hypertrophic response to PH (70) is not replaced by a response of proliferation but may occur simultaneously around POD 1. We add new knowledge to the field of Miyaoka et al and report the dynamics of hepatocyte hypertrophy and proliferation after the extensive PH (90). Our results suggest that the hypertrophic dynamics after PH (90) follows that of minor PHs with an early increase and peak at POD 1; however, the more pronounced the bigger PH. The second proliferative response to major PH suggested by Miyaoka et al may in our study be the case after PH (90)—not absolutely after PH (70).

In conclusion, general hypertrophy of hepatocytes after different size of PH was followed by hepatocyte proliferation only in the liver remnant of PH (70) and PH (90).

Understanding the mechanisms of liver regeneration following PH is important to potentially improve outcome after curative intended PH for liver malignancy. In this study, we present new knowledge on the hypertrophic and hyperplastic regenerative dynamics of the 10% MSFLR on the brink of liver failure. It may be important knowledge for future studies to take into account trying to understand the mechanisms of the regenerative process in general and the recovering and survival after extensive PH and potential liver failure in specific.

ACKNOWLEDGEMENTS

The authors thank Stine Hasselholt, Helene Andersen, Gitte Brix and Tine Meyer for their excellent technical assistance. Centre for Stochastic Geometry and Advanced Bioimaging is supported by Villum Foundation.

CONFLICT OF INTERESTS

The authors have no conflict of interests or pertinent financial relationships to declare.

AUTHOR CONTRIBUTIONS

Michelle Meier designed the study, carried out the surgical procedures, collected and analysed the data and wrote the manuscript. Kasper Jarlhelt Andersen designed the study, participated in surgical procedure consultancy, collected and analysed the data and wrote the manuscript. Anders Riegels Knudsen designed the study, participated in surgical procedure consultancy, analysed the data and drafted the manuscript. Jens Randell Nyengaard designed the study and participated in stereological consultancy. Stephen Hamilton-Dutoit designed the study and participated in histological consultancy. Fran Viborg Mortensen designed the study, analysed the data and wrote the manuscript.

ORCID

Kasper Jarlhelt Andersen http://orcid.org/0000-0002-5290-7515

REFERENCES

1. Lintoiu-Ursut B, Tulin A, Constantinoiu S. Recurrence after hepatic resection in colorectal cancer liver metastasis -Review article. *J Med Life* 2015;8:12-14. Spec Issue.
2. Parkin DM, Bray F, Ferlay J, Pisani P. Global cancer statistics, 2002. *CA Cancer J Clin*. 2005;55:74-108.
3. Hyder O, Pulitano C, Firoozmand A, et al. A risk model to predict 90-day mortality among patients undergoing hepatic resection. *J Am Coll Surg*. 2013;216:1049-1056.
4. Gaub J, Iversen J. Rat liver regeneration after 90% partial hepatectomy. *Hepatology*. 1984;4:902-904.
5. Madrahimov N, Dirsch O, Broelsch C, Dahmen U. Marginal hepatectomy in the rat: from anatomy to surgery. *Ann Surg*. 2006;244:89-98.
6. Michalopoulos GK. Principles of liver regeneration and growth homeostasis. *Compr Physiol*. 2013;3:485-513.
7. Conlon I, Raff M. Size control in animal development. *Cell*. 1999;96:235-244.
8. Miyaoka Y, Ebato K, Kato H, Arakawa S, Shimizu S, Miyajima A. Hypertrophy and unconventional cell division of hepatocytes underlie liver regeneration. *Curr Biol*. 2012;22:1166-1175.
9. Andersen KJ, Knudsen AR, Kannerup AS, et al. The natural history of liver regeneration in rats: description of an animal model for liver regeneration studies. *Int J Surg*. 2013;11:903-908.
10. Meier M, Andersen KJ, Knudsen AR, Nyengaard JR, Hamilton-Dutoit S, Mortensen FV. Liver regeneration is dependent on the extent of hepatectomy. *J Surg Res*. 2016;205:76-84.
11. Muhlfeld C, Nyengaard JR, Mayhew TM. A review of state-of-the-art stereology for better quantitative 3D morphology in cardiac research. *Cardiovasc Pathol*. 2010;19:65-82.
12. Nyengaard JR. Stereologic methods and their application in kidney research. *J Am Soc Nephrol*. 1999;10:1100-1123.
13. Scholzen T, Gerdes J. The Ki-67 protein: from the known and the unknown. *J Cell Physiol*. 2000;182:311-322.
14. Rasmusson A, Hahn U, Larsen JO, Gundersen HJG, Jensen EBV, Nyengaard JR. The spatial rotator. *J Microsc*. 2013;250:88-100.
15. Hosseini-Sharifabad M, Nyengaard JR. Design-based estimation of neuronal number and individual neuronal volume in the rat hippocampus. *J Neurosci Methods*. 2007;162:206-214.
16. Inderbitzin D, Studer P, Sidler D, et al. Regenerative capacity of individual liver lobes in the microsurgical mouse model. *Microsurgery*. 2006;26:465-469.
17. Kim RD, Stein GS, Chari RS. Impact of cell swelling on proliferative signal transduction in the liver. *J Cell Biochem*. 2001;83:56-69.
18. Higgins GM, Anderson RM. Experimental pathology of the liver: restoration of the liver of the white rat following partial surgical removal. *Arch Pathol*. 1931;12:186-202.
19. Boyce RW, Dorph-Petersen KA, Lyck L, Gundersen HJ. Design-based stereology: introduction to basic concepts and practical approaches for estimation of cell number. *Toxicol Pathol*. 2010;38:1011-1025.
20. Hoekstra LT, de Graaf W, Nibourg GA, et al. Physiological and biochemical basis of clinical liver function tests: a review. *Ann Surg*. 2013;257:27-36.
21. Collier J, Bassendine M. How to respond to abnormal liver function tests. *Clin Med (Lond)*. 2002;2:406-409.
22. Schmidt E, Schmidt FW. Enzyme diagnosis of liver diseases. *Clin Biochem*. 1993;26:241-251.
23. Poulsen HE, Gaub J, Iversen J. Changes in quantitative measures of hepatic function after 90% hepatectomy in rats. *Eur J Clin Invest*. 1985;15:285-9.

How to cite this article: Meier M, Andersen KJ, Knudsen AR, Nyengaard JR, Hamilton-Dutoit S, Mortensen FV. Adaptive growth changes in the liver remnant are affected by the size of hepatectomy in rats. *Int J Exp Path*. 2018;99:150–157. https://doi.org/10.1111/iep.12282